

Synthesis and Characterization of a New Ternary Imide— $\text{Li}_2\text{Ca}(\text{NH})_2$ Guotao Wu,<sup>†</sup> Zhitao Xiong,<sup>†</sup> Tao Liu,<sup>†</sup> Yongfeng Liu,<sup>†</sup> Jianjiang Hu,<sup>†</sup> Ping Chen,<sup>\*,†,‡</sup>  
Yuanping Feng,<sup>†</sup> and Andrew T. S. Wee<sup>†</sup>

Department of Physics and Department of Chemistry, National University of Singapore, 10 Kent Ridge Crescent, Singapore 117542

Received May 6, 2006

The ternary imide  $\text{Li}_2\text{Ca}(\text{NH})_2$  was successfully synthesized by dehydrogenating a mixture of  $\text{LiNH}_2$  and  $\text{CaH}_2$  at a molar ratio of 2:1 in a stream of purified argon at 300 °C. A powder X-ray diffraction measurement revealed that  $\text{Li}_2\text{Ca}(\text{NH})_2$  was of the trigonal anti- $\text{La}_2\text{O}_3$  structure (space group  $\bar{P}3m1$ ) with lattice constants of  $a = 3.5664(3)\text{Å}$  and  $c = 5.9540(8)\text{Å}$ . Ca occupied the 1b site (0, 0, 1/2), Li occupied the 2d site (1/3, 2/3, 0.8841(22)), and N occupied the 2d site (1/3, 2/3, 0.2565(15)). Nuclear magnetic resonance and X-ray absorption fine structure analyses demonstrated that each Li ion was coordinated with four imide ions and each Ca ion was coordinated with six imide ions.

## Introduction

Binary nitrides, amides, and imides of various metals and nonmetals have been well studied by Juza and co-workers since the 1920s.<sup>1</sup> These compounds have many interesting properties that make them attractive for technological applications. Binary nitrides (e.g., GaN, InN, AlN, BN, and TiN) have a number of applications in the microelectronic, optoelectronic, abrasion, and corrosion protection industries.<sup>2–4</sup> Binary amides, such as lithium and sodium amides, are widely used as deprotonating agents in organic synthesis.<sup>5</sup> Recently, lithium nitride and lithium imide were found to exhibit strong affinity to  $\text{H}_2$ , which enable them to be potential candidates for hydrogen storage.<sup>6,7</sup> Rapid growth in nitride chemistry occurred in the last decades owing to the improved classification of nitride crystal chemistry and the development of new synthetic techniques, leading to the discovery of a wide range of new ternary compounds with

diverse crystal structures and interesting physical properties.<sup>1–4</sup> Recent investigations on synthesis methods, structures, and properties of ternary and higher nitrides were summarized by Gregory and Niewa et al., respectively.<sup>2–4</sup> However, research in ternary and higher inorganic imides is rare. It was only in recent years that ternary imides containing both an alkaline metal and an alkaline earth metal were synthesized and investigated.<sup>8,9</sup> As an example,  $\text{Li}_2\text{Mg}(\text{NH})_2$  can be synthesized by reacting  $\text{LiNH}_2$  with  $\text{MgH}_2$  at elevated temperatures.<sup>8,9</sup> Synchrotron X-ray diffraction (XRD) and neutron diffraction measurements reveal that  $\text{Li}_2\text{Mg}(\text{NH})_2$  possesses three different crystal structures depending on the synthesis temperature.<sup>10</sup> A similar synthetic route was applied to the Li–Ca–N–H system, but little attention was paid to its structural identification and chemical properties.<sup>8</sup> If the structure of  $\text{Li}_2\text{Ca}(\text{NH})_2$  is determined, the physical and chemical properties of this new ternary imide can be well predicted and understood by theoretical means.<sup>11,12</sup>

Systematic studies of amides and imides were performed by Juza et al., Jacobs and Schmidt, and Rouxel et al. previously.<sup>13–17</sup> Normally, imides (e.g.,  $\text{Li}_2\text{NH}$ ,  $\text{CaNH}$ , and  $\text{BaNH}$ ) are prepared by heating amides under vacuum.<sup>13–15</sup>

\* To whom correspondence should be addressed. Fax: +65-67776126. Tel.: +65-65165100. E-mail: phychenp@nus.edu.sg.

<sup>†</sup> Department of Physics.

<sup>‡</sup> Department of Chemistry.

- (1) Brese, N. E.; O'Keeffe, M. *Struct. Bonding (Berlin)* **1992**, 79, 307–378.
- (2) Gregory, D. H. *J. Chem. Soc., Dalton Trans.* **1999**, 3, 259–270.
- (3) Niewa, R.; Jacobs, H. *Chem. Rev.* **1996**, 96, 2053.
- (4) Niewa, R.; DiSalvo, F. J. *Chem. Mater.* **1998**, 10, 2733–2752.
- (5) Erden, I. In *Handbook of Reagents for Organic Synthesis: Acidic and Basic Reagents*; Reich, H. J., Rigby, J. H., Eds.; Wiley: Chichester, U.K., 1999; p 204.
- (6) Chen, P.; Xiong, Z. T.; Luo, J. Z.; Lin, J. Y.; Tan, K. L. *Nature* **2002**, 420, 302–304.
- (7) Chen, P.; Xiong, Z. T.; Luo, J. Z.; Lin, J. Y.; Tan, K. L. *J. Phys. Chem. B* **2003**, 107, 10967–10970.
- (8) Xiong, Z. T.; Wu, G. T.; Hu, J. J.; Chen, P. *Adv. Mater.* **2004**, 16, 1522–1525.
- (9) Luo, W. F. *J. Alloys Compd.* **2004**, 381, 284–287.
- (10) Zhao, J. C. Phase formation and reaction pathway of  $\text{Mg}(\text{NH}_2)_2 + 2\text{LiH}$  mixture for reversible hydrogen storage. Presented at the International Partnership for the Hydrogen Economy, Jucca, Italy, June 19–22, 2005.
- (11) Zhao, J. C.; Dyer, M.; Alavi, A. *J. Phys. Chem. B* **2005**, 109, 22089–22091.
- (12) Herbst, J. F.; Hector, L. G. *Phys. Rev. B* **2005**, 72, 125120.
- (13) Juza, R.; Opp, K. Z. *Anorg. Allg. Chem.* **1951**, 266, 313–324.

However, because of the lack of ternary amides, few ternary imides have been synthesized and reported in the literature.<sup>13–17</sup> The novel synthetic route involving reaction of a binary amide with a hydride under appropriate conditions has proven to be a viable method for making a variety of novel ternary imides.<sup>8,9</sup> In this paper, the synthetic approach mentioned above was applied to the preparation of the ternary imide of  $\text{Li}_2\text{Ca}(\text{NH})_2$ . The synthesis was carried out at relatively low temperatures because of the poor thermal stability of  $\text{Li}_2\text{Ca}(\text{NH})_2$ . As a consequence, only microcrystalline imides may be obtained. Determination of the structure merely by powder XRD alone may not be sufficiently accurate. Therefore, combined characterizations by means of XRD, vibrational spectra, X-ray absorption spectra, and nuclear magnetic resonance (NMR) were performed to acquire structural information on both the bulk and the atomic scales with the intention of obtaining a better understanding of the composition, structure, and properties of  $\text{Li}_2\text{Ca}(\text{NH})_2$ .

## Experimental Section

**Preparation of  $\text{Li}_2\text{Ca}(\text{NH})_2$ .**  $\text{LiNH}_2$  and  $\text{CaH}_2$  were synthesized by reacting metallic Li (99.9%, Aldrich Chemicals) with ammonia (99.98%, BOC Gases) and by reacting metallic Ca (99.9%, Aldrich Chemicals) with hydrogen (99.99%, National Oxygen), respectively.  $\text{LiNH}_2$  and  $\text{CaH}_2$  at a molar ratio of 2:1 were thoroughly mixed by a SPEX 8000M mixer/mill.  $\text{Li}_2\text{Ca}(\text{NH})_2$  was synthesized by heating the post-milled mixture in a flow of purified argon from room temperature to 300 °C at a ramping rate of 1 °C/min. Gaseous products were analyzed by an on-line HPR20 mass spectrometer (MS) in tandem with a gas chromatograph (GC). For the quantitative analysis of ammonia, gaseous products were slowly introduced to distilled water. A Metrohm 781 pH/ion meter equipped with an  $\text{NH}_3$ -selective electrode was used to detect the concentration of ammonia in distilled water. A quantitative measurement of hydrogen desorption was conducted in a commercial pressure composition isotherm (PCI) unit from Advanced Materials Corporation.

**Structure Determination.** XRD data were collected using a BRUKER D8 Advance X-ray diffractometer with Cu K $\alpha$  radiation at a power of 40 kV  $\times$  40 mA. Stepwise scans were performed in the  $2\theta$  range of 10–90° at steps of 0.05°. The obtained data were indexed using the TREOR or DICVOL program. Lattice parameters were refined by a least-squares refinement method using the CELREF program. Rietveld refinement structural analyses were performed using the Rietica program.<sup>18</sup>

N–H vibration was recorded using a Perkin-Elmer Fourier transform infrared (FTIR) spectroscopy 2000 spectrometer equipped with a diffuse reflectance infrared Fourier transform (DRIFT) cell. The scan range was 400–4000  $\text{cm}^{-1}$ , and the resolution was 4  $\text{cm}^{-1}$ .

Transmission X-ray absorption fine structure (XAFS) spectra were collected in the vicinity of the Ca K edge (4.038 keV) at room temperature at the XDD beamline of the Singapore Synchrotron Light Source (SSLS, Singapore).<sup>19</sup> Each sample was ground and mixed with LiF powder (99%, Fluka) at a weight ratio of 1:10. The mixture was pressed into a pellet under a pressure of 2.5 tons

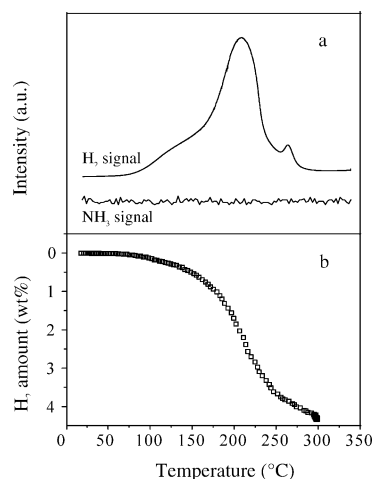


**Figure 1.** TPD (a) and volumetric release (b) measurements on the post-milled  $2\text{LiNH}_2\text{--CaH}_2$  samples.

and then coated with solid wax in the glovebox to avoid air contamination during XAFS measurements. The sample thickness was adjusted to achieve the X-ray absorption edge jump of approximately one for each sample.

Analysis of the XAFS data followed the standard procedures using the WINXAS code.<sup>20</sup> After normalization, transformation from energy space to momentum ( $k$ ) space, and extraction of the background absorption were carried out, the  $\chi(k)$  function was extracted in the range of 2.2–9.2  $\text{\AA}^{-1}$  and weighted by  $k^3$ . Fourier transform of  $k^3\chi(k)$  into  $R$  space was performed using the Bessel function. The data fit of the first coordination shell was performed using  $\text{CaNH}$  as the reference.

$^6\text{Li}$  magic-angle spinning (MAS) NMR measurements were carried out at room temperature in a Bruker Advance 400 spectrometer with a 4 mm broadband cross-polarization (CP)/MAS probe operating at a  $^6\text{Li}$  frequency of 58.8 MHz. Each sample was packed in a zirconia rotor with a Kel-F cap and rotated at a rotor-spinning rate of 10 kHz. Chemical shifts were reported with respect to a 1 M LiCl aqueous solution. The peaks in the NMR spectra were fitted to obtain the values of the full width at half-maximum and chemical shift.

As the starting materials and products were sensitive to air, all sample loadings were performed in an MBRAUN glovebox. The glovebox was filled with purified argon gas. Water and oxygen concentrations were below 10 ppm.

## Results and Discussion

Temperature programmed desorption (TPD) of the post-milled  $2\text{LiNH}_2 + \text{CaH}_2$  sample was performed by using purified argon as a carrier gas. The temperature was raised from room temperature to 300 °C at a ramping rate of 1 °C/min. The sample (100.2 mg) was loaded, and plots of temperature versus the mass spectrometer signals of the outlet gas were obtained (Figure 1a). Ammonia was undetectable by MS during the whole testing period, indicating that the amount of coproduced ammonia was negligible. Notably, the

(14) Juza, R.; Schumacher, H. Z. *Anorg. Allg. Chem.* **1963**, 324, 278–286.

(15) Jacobs, H.; Schmidt, D. *Curr. Top. Mater. Sci.* **1982**, 8, 381–427.

(16) Brec, R.; Rouxel, J. C. R. *Acad. Sci. Palls. Ser. C* **1967**, 264, 512–515.

(17) Palvadeau, P.; Rouxel, J. *Bull. Soc. Chim. Fr.* **1970**, 2, 480–485.

(18) All of the programs download from <http://www.ccp14.ac.uk>.

(19) Moser, H. O.; Casse, B. D. F.; Chew, E. P.; Cholewa, M.; Diao, C. Z.; Ding, S. X. D.; Kong, J. R.; Li, Z. W.; Hua, M.; Ng, M. L.; Saw, B. T.; bin Mahmood, S.; Vidyaraj, S. V.; Wilhelmi, O.; Wong, J.; Yang, P.; Yu, X. J.; Gao, X. Y.; Wee, A. T. S.; Sim, W. S.; Lu, D.; Faltermeyer, R. B. *Nucl. Instrum. Methods Phys. Res., Sect. B* **2005**, 238, 83–86.

(20) Ressler, T. J. *J. Phys. IV* **1997**, 7, 269–270.

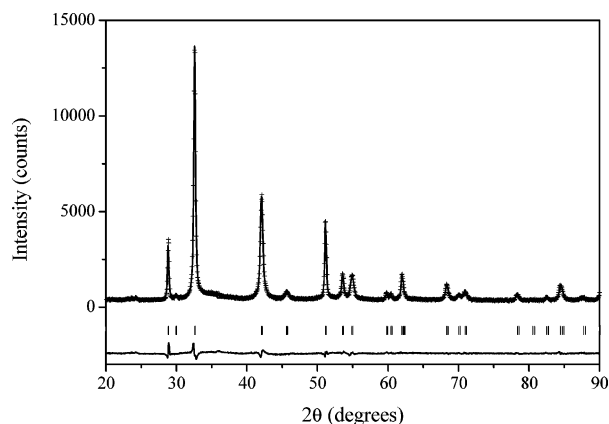


**Figure 2.** XRD patterns of the ternary imide  $\text{Li}_2\text{Ca}(\text{NH})_2$ . Legend: +, observed; −, calculated; bottom line, the difference; and vertical tick, Bragg peak positions.

$\text{NH}_3$  concentration in the desorbed hydrogen was below 100 ppm according to the amount of ammonia detected by the Metrohm 781 pH/ion meter. Hydrogen appeared at temperatures above 50 °C and peaked at 140 °C and 206 °C. After the dehydrogenation, 95.7 mg of the solid residue was obtained, indicating a release of 4.5 mg of hydrogen which was equivalent to  $\sim 4.0$  H atoms per  $2\text{LiNH}_2 + \text{CaH}_2$ . Volumetric measurement of the amount of hydrogen desorbed during the thermal treatment also gave a similar result. As shown in Figure 1b, about 4.3 wt % of hydrogen was released from the starting materials, which was equivalent to 3.8 H atoms per  $2\text{LiNH}_2 + \text{CaH}_2$ . The slight difference between the results from these two aforementioned methods may be due to differences in the hydrogen pressure in the two testing systems. In the TPD measurement, the partial pressure of  $\text{H}_2$  in the gaseous phase was negligible. However, in the volumetric release measurement, hydrogen was gradually accumulated in the sample chamber, reaching 0.3 bar at the end of the test. Part of the hydrogen could not be released because of the reaction equilibrium limit. On the basis of the amount of hydrogen detached from the starting chemicals, the chemical composition of the dehydrogenated solid product should be  $\text{Li}_2\text{CaN}_2\text{H}_2$ . The rehydrogenation of the solid residue was achieved when applying 80 bar of hydrogen to the sample in the temperature range of 20 to 200 °C.<sup>8</sup>

The dehydrogenated solid product was characterized by XRD and identified by searching and matching the JCPDS-ICDD cards. The characteristic diffraction peaks of the starting amide and hydride disappeared (Figure 2). Instead, a new set of peaks positioned at 32.5°, 42.1°, 51.1°, and so forth emerged, which could not be matched with any known compounds containing Li, Ca, N, and H elements.<sup>8</sup> After indexing with the TREOR program, the XRD pattern of the solid product matched well with a single phase having the hexagonal structure with lattice constants of  $a = 3.566$  Å and  $c = 5.954$  Å. To be a neutral molecule, H in the  $\text{Li}_2\text{CaN}_2\text{H}_2$  phase should be positively charged and bond with N. Therefore, this newly developed compound is a new ternary imide, represented by  $\text{Li}_2\text{Ca}(\text{NH})_2$ .

Rietveld refinement of the XRD data was performed by using a structure model containing  $\text{Li}^+$ ,  $\text{Ca}^{2+}$ , and  $\text{N}^{3-}$ .

**Table 1.**  $\text{Li}_2\text{Ca}(\text{NH})_2$  Crystallographic Data<sup>a</sup>

space group	$P\bar{3}m1$			
unit cell dimensions	$a = 3.5664(3)$ Å, $c = 5.9540(8)$ Å			
cell volume	$V = 65.585(11)$ Å <sup>3</sup>			
Z, density	$Z = 1$ , $d = 2.126$ g/cm <sup>3</sup>			
atom	position	x	y	z
Ca	1b	0	0	0.5
Li	2d	1/3	2/3	0.8841(22)
N	2d	1/3	2/3	0.2565(15)
H	not included			
Interatomic Distances				
Ca–N	$2.518$ Å $\times 6$	Li–N	$2.223$ Å $\times 3$	$2.217$ Å $\times 1$
Li–Li	$2.479$ Å	Ca–Ca	$3.566$ Å	
Li–Ca	$3.077$ Å			

<sup>a</sup>  $R_p = 7.37\%$ ,  $R_{wp} = 9.54\%$ .

Because the scattering factor of hydrogen is very small compared to those of the other elements, hydrogen has little effect on XRD and can therefore be neglected. In order to locate hydrogen, neutron diffraction of a deuterium-substituted sample should be performed.  $\text{Li}^+$ ,  $\text{Ca}^{2+}$ , and  $\text{N}^{3-}$  positions in the initial model for Rietveld refinement were derived from published structures of ternary nitrides. Ternary lithium nitrides can be divided mainly into two groups, that is, those with anti-fluorite type crystal structures represented by a general formula  $\text{Li}_{2n-3}\text{M}^{n+}\text{N}_{n-1}$  ( $n \geq 2$ ) and those with the anti- $\text{La}_2\text{O}_3$  type structure represented by a general formula  $\text{Li}_2\text{MN}_2$ .<sup>1</sup> As evidenced by the indexing result of the TREOR program,  $\text{Li}_2\text{Ca}(\text{NH})_2$  should possess the anti- $\text{La}_2\text{O}_3$  type structure, which belongs to the hexagonal structure.  $\text{CaMg}_2\text{N}_2$  (JCPDS-ICDD card no. 83–0042)<sup>21</sup> has the anti- $\text{La}_2\text{O}_3$  type structure with lattice constants of  $a = 3.5405$  Å and  $c = 6.0908$  Å. Since the ionic radii of  $\text{Li}^+$  and  $\text{Mg}^{2+}$  are almost identical (0.68 and 0.67 Å),<sup>22</sup> the structure of  $\text{CaMg}_2\text{N}_2$  was adopted as the starting model to study  $\text{Li}_2\text{Ca}(\text{NH})_2$ , wherein  $\text{Mg}^{2+}$  was substituted by  $\text{Li}^+$ . The experimental powder XRD pattern of  $\text{Li}_2\text{Ca}(\text{NH})_2$  was in excellent agreement with the calculated pattern derived from the starting model (Figure 2), which implied that the structural model adopted in the present simulation was reasonable and acceptable. A series of parameters, including background, zero shift, scale, lattice parameter, graphic parameter (U, V, W), and Li and N coordinates, were refined by the Rietica program (Table 1).  $\text{Li}_2\text{Ca}(\text{NH})_2$  belongs to the space group  $P\bar{3}m1$  with lattice constants of  $a = 3.5664(4)$  Å and  $c = 5.9540(8)$  Å. Ca occupies the 1b site (0, 0, 1/2), Li occupies the 2d site (1/3, 2/3, 0.8841(22)), and N occupies the 2d site (1/3, 2/3, 0.2565(15)). The regular octahedral and tetrahedral holes of the approximately cubic closed-packed matrix of nitrogen in the  $\text{Li}_2\text{Ca}(\text{NH})_2$  lattice (Figure 3) are the occupation sites for Ca and Li, respectively.

High-resolution  $^6\text{Li}$  MAS NMR was employed to study the chemical environment of Li in the ternary imide. The chemical shift values are directly related to the shielding of the nucleus by the electronic structure of its local environ-

(21) Schultz-Coulon, V.; Schnick, W. *Z. Naturforsch., B: Chem. Sci.* **1995**, *50*, 619–622.

(22) Juza, R.; Langer, K.; von Benda, K. *Angew. Chem., Int. Ed. Engl.* **1968**, *7*, 360–370.

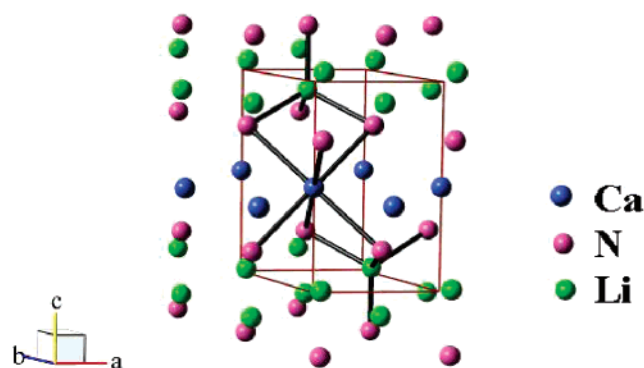


**Figure 3.** Crystal structure of the ternary imide  $\text{Li}_2\text{Ca}(\text{NH})_2$ . Li, green spheres; Ca, blue spheres; N, purple spheres. The unit cell is delineated by the dark yellow line. Li and Ca are linked to N coordinates by black sticks.

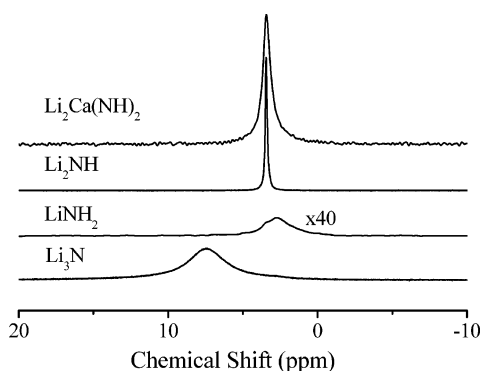


**Figure 4.** Solid state  $^6\text{Li}$  MAS NMR spectra of  $\text{Li}_2\text{Ca}(\text{NH})_2$ ,  $\text{Li}_2\text{NH}$ ,  $\text{LiNH}_2$ , and  $\text{Li}_3\text{N}$ .

ment.<sup>23</sup> For example, there is a proportional correlation between the  $^6\text{Li}$  chemical shifts and the oxygen coordination number in lithium silicate.<sup>23</sup> As shown in Figure 4, Li in  $\text{Li}_2\text{Ca}(\text{NH})_2$ ,  $\text{Li}_2\text{NH}$ ,  $\text{Li}_3\text{N}$ , and  $\text{LiNH}_2$  has the chemical shifts of 3.433, 3.455, 7.493, and 2.748 ppm, respectively. Similar chemical shifts of Li in  $\text{Li}_2\text{Ca}(\text{NH})_2$  and  $\text{Li}_2\text{NH}$  indicate the identical chemical environment of Li in these two compounds.  $\text{Li}_2\text{NH}$  has a simple face-centered cubic (fcc) structure with  $Fm\bar{3}m$  symmetry.<sup>13</sup> Each lithium cation in  $\text{Li}_2\text{NH}$  is coordinated with four imide anions. It is likely that the coordination number of the lithium cation in  $\text{Li}_2\text{Ca}(\text{NH})_2$  is the same as that in  $\text{Li}_2\text{NH}$ , in agreement with the XRD results.

X-ray absorption near-edge structure (XANES) spectroscopy is a powerful technique in determining metal atom/ion coordination number, especially when an appropriate model compound with well-defined coordination structure is available for comparison. In the present study,  $\text{Ca}_3\text{N}_2$  was used as the reference for Ca in tetrahedral coordination,<sup>24</sup> and  $\text{CaNH}$  was used as the reference for Ca in octahedral coordination.<sup>14,25</sup> Figure 5 shows the XANES spectra of  $\text{Ca}_3\text{N}_2$ ,  $\text{CaNH}$ , and  $\text{Li}_2\text{Ca}(\text{NH})_2$  samples at the Ca K edge. The peak at 4.050 keV is ascribed to the Ca 1s to 4p dipole transition. The peak at 4.038 keV is the pre-edge transition,

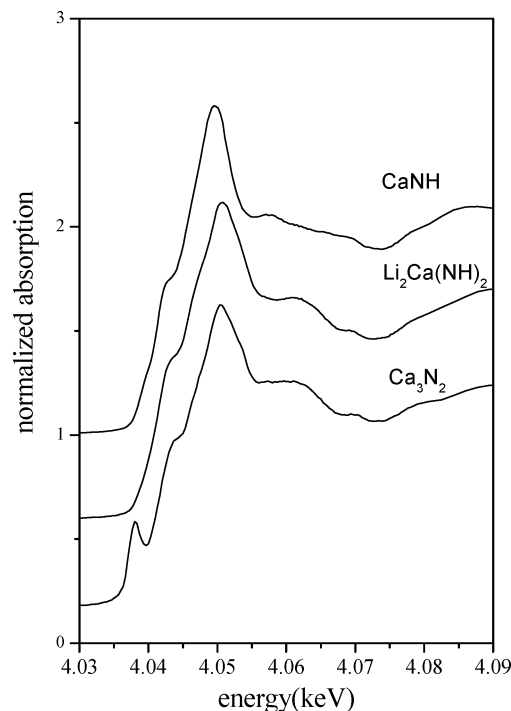


**Figure 5.** XANES transmission spectra at the Ca K edge of the  $\text{Ca}_3\text{N}_2$ ,  $\text{CaNH}$ , and  $\text{Li}_2\text{Ca}(\text{NH})_2$  samples.

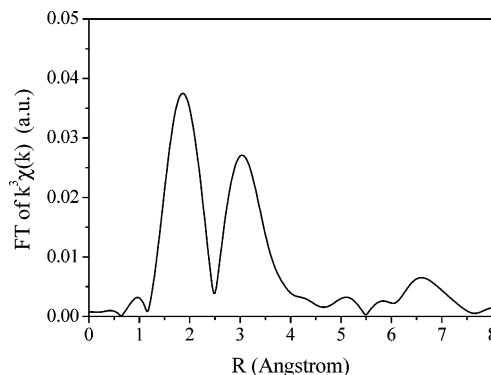


**Figure 6.** Fourier transforms of the EXAFS spectra of ternary imide  $\text{Li}_2\text{Ca}(\text{NH})_2$ .

which is related to the direct 1s to 3d quadrupole transition or the dipole transitions due to the d–p mixing between the 3d orbitals and the 4p orbitals of the central atom or neighboring atoms.<sup>26,27</sup> Therefore, the intensities of the pre-edge features are sensitive to the local coordination geometry of the metal atom.<sup>26,27</sup> It can be seen in Figure 5 that the intensity of the peak at 4.038 keV is much higher for Ca in the tetrahedral site than that in the octahedral site. Similar to that of  $\text{CaNH}$ , the intensity of the peak at 4.038 keV for  $\text{Li}_2\text{Ca}(\text{NH})_2$  is very weak, indicating an octahedral coordination.

The Fourier transform of the extended XAFS (EXAFS) spectrum for  $\text{Li}_2\text{Ca}(\text{NH})_2$  is presented in Figure 6. The peak at the radial distance of about 2.0 Å corresponds to the above-mentioned Ca–N coordination of the first shell. For the data evaluation, the peak between 1 Å and 2.5 Å was isolated by

(23) Xu, Z.; Stebbins, J. F. *Solid State Nucl. Magn. Reson.* **1995**, *5*, 103–112.

(24) Heyns, A. M.; Prinsloo, L. C.; Range, K. J.; Stassen, M. J. *Solid State Chem.* **1998**, *137*, 33–41.

(25) Sichla, T.; Jacobs, H. Z. *Anorg. Allg. Chem.* **1996**, *622*, 2079–2082.

(26) Chen, L. X.; Liu, T.; Thurnauer, M. C.; Csencsits, R.; Rahj, T. J. *Phys. Chem. B* **2002**, *106*, 8539–8546.

(27) de Groot, F. *Chem. Rev.* **2001**, *101*, 1779–1808.



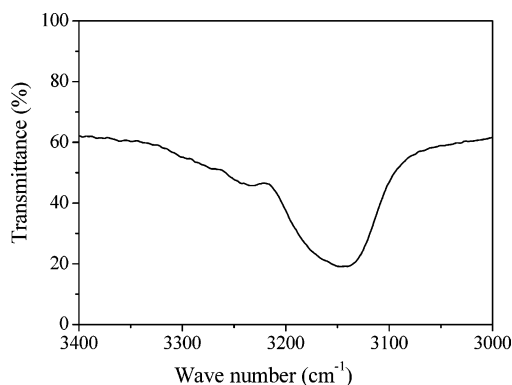


**Figure 7.** FTIR spectra of the ternary imide  $\text{Li}_2\text{Ca}(\text{NH})_2$ .

means of a filter function, and fitted with the amplitude reduction factor of  $S_0^2 = 0.73$ . The value of 0.73 is derived from the fitting results of the EXAFS data of  $\text{CaNH}$  using the coordination number and distance of the first shell from crystallographic data.<sup>14,25</sup> The coordination number of Ca obtained from the EXAFS data of  $\text{Li}_2\text{Ca}(\text{NH})_2$  is 6.3, which indicates that each Ca is coordinated with six N, in good agreement with the XRD results.

To investigate the position of H in the lattice and the nature of the N–H bond,  $\text{Li}_2\text{Ca}(\text{NH})_2$  was further analyzed by FTIR spectroscopy. A broad absorbance in the range of  $3050\text{ cm}^{-1}$  to  $3200\text{ cm}^{-1}$  was detected (Figure 7), which correlates with the stretch of the N–H bond in imide ions.<sup>7,28</sup> For example, N–H stretches in  $\text{Li}_2\text{NH}$  and  $\text{CaNH}$  are  $3160\text{ cm}^{-1}$  and  $3183\text{ cm}^{-1}$ , respectively.<sup>7,28</sup> The broad peak is characteristic of imide ions, which may be the result of dynamic or static disorder of hydrogen over the equivalent sites that broadens the localized vibrational states into bands.<sup>11,25</sup> The overall absorbance of the ternary imide resembles that of  $\text{Li}_2\text{NH}$  except the asymmetric nature caused by the presence of Ca. Thus, the hydrogen site in  $\text{Li}_2\text{Ca}(\text{NH})_2$  can refer to that in the  $\text{Li}_2\text{NH}$  lattice. In the crystal structure model of  $\text{Li}_2\text{NH}$ , the hydrogen site is 16e ( $F\bar{4}3m$ ) or 48h ( $Fm\bar{3}m$ ).<sup>29</sup> The recent neutron diffraction and XRD results and the DFT calculations revealed that  $\text{Li}_2\text{ND}$  can have a disordered cubic ( $Fd\bar{3}m$ ) structure with partially occupied Li 32e sites below 360 K and have the disordered cubic ( $Fm\bar{3}m$ ) structure with D atoms

randomized over the 192i sites above that temperature.<sup>30</sup> According to the  $^1\text{H}$  NMR measurement result of the solid lithium imide, the N–H vector is oriented to the middle point of two adjacent lithium sites.<sup>31</sup> The first-principles calculations based on the density functional theory (DFT) were used to identify H positions in  $\text{Li}_2\text{Ca}(\text{NH})_2$  (details in Supporting Information). Our detailed DFT calculations on  $\text{Li}_2\text{Ca}(\text{NH})_2$  reveal that H atoms may distribute over the 6i equivalent sites (0.1838, 0.8162, 0.1723) around nitrogen atoms, and the N–H vector orients toward the middle point of two adjacent lithium sites (Li–Li distance  $3.566\text{ \AA}$ ). Further investigations by neutron powder diffraction, NMR, and neutron inelastic scattering are needed to provide more information on the position and dynamics of hydrogen in  $\text{Li}_2\text{Ca}(\text{NH})_2$ .

## Conclusions

Thermal dehydrogenation of a mixture of  $\text{LiNH}_2$  and  $\text{CaH}_2$  at a molar ratio of 2:1 led to the formation of a new ternary imide  $\text{Li}_2\text{Ca}(\text{NH})_2$ . The crystal structure of  $\text{Li}_2\text{Ca}(\text{NH})_2$  was determined by powder XRD. It adopts the trigonal anti- $\text{La}_2\text{O}_3$  structure (space group  $P\bar{3}m1$ ). The cell parameters and atomic fractional coordinates were refined by the Rietveld method. Furthermore, local coordination states around Li and Ca in the  $\text{Li}_2\text{Ca}(\text{NH})_2$  crystal were investigated by  $^6\text{Li}$  MAS NMR and by XAFS at the Ca K edge, respectively, and the results were in good agreement with the results of the XRD measurement.

**Acknowledgment.** The present work is financially supported by the Agency of Science, Technology, and Research, Singapore (A\*STARS). Work of XAFS was performed at Singapore Synchrotron Light Source (SSLS) under NUS Core Support C-380-003-003-001, A\*STAR/MOE RP 3979908M, and Grant A\*STAR 12 105 0038. We thank Dr. Ping Yang for the technical support at the XDD beamline.

**Supporting Information Available:** H positions in  $\text{Li}_2\text{Ca}(\text{NH})_2$  were investigated by the first-principles calculations based on the density functional theory (DFT). This material is available free of charge via the Internet at <http://pubs.acs.org>.

IC060769Y

(28) Linde, G.; Juza, R. Z. *Anorg. Allg. Chem.* **1974**, 409, 119–214.

(29) Ohoyama, K.; Nakamori, Y.; Orimo, S.; Yamada, K. *J. Phys. Soc. Jpn.* **2005**, 74, 483–487.

(30) Balogh, M. P.; Jones, C. Y.; Herbst, J. F.; Hector, L. G.; Kundrat, M. *J. Alloys Compd.* **2006**, 420, 326–336.

(31) Haigh, P. J.; Forman, R. A.; Frisch, R. C. *J. Chem. Phys.* **1966**, 45, 812–816.